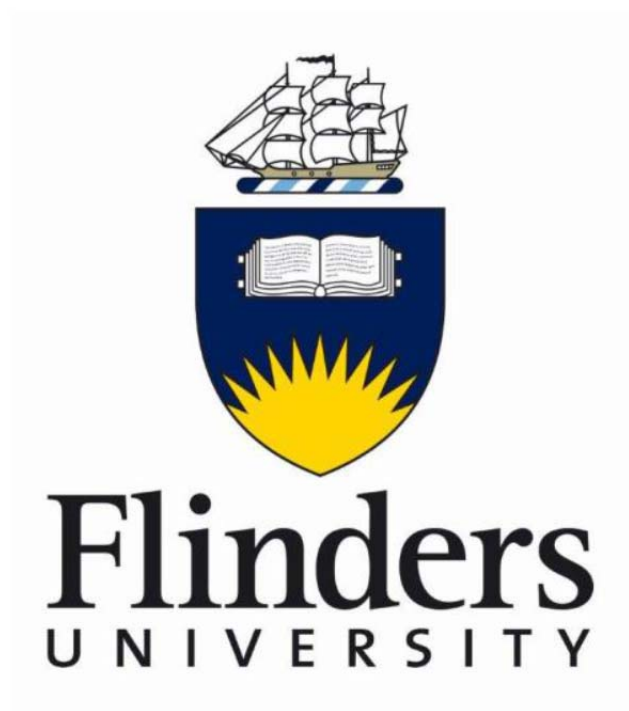


Investigating the Surface Structure of Liquids Containing Ionic Species



Christiaan Ridings

Thesis submitted to the School of Chemical and Physical Sciences,

Faculty of Science and Engineering

Flinders University

in fulfilment of the requirements for the degree of

Doctor of Philosophy

October 2014

Table of contents

Abstract	i
Declaration	iii
Acknowledgements	v
List of Publications	vii
List of Figures	ix
List of Tables	xv
Abbreviations	xvi
Contextual Statement	xix
Chapter 1: Introduction	1
1.1 Overview	1
1.2 Liquid surfaces	2
1.2.1 Surface structure in liquids	2
1.2.2 Surface charge of liquids	5
1.2.3 DLVO theory	9
1.2.4 Specific ion effects	11
1.3 Surfactants and Foam Films	12
1.3.1 Disjoining pressure	13
1.3.2 Foam film stability	14
1.3.3 Common black and Newton black films	15
1.3.4 Thin foam film structure	17
1.3.5 Specific ion effects in foams and foam films	19
1.4 Ionic Liquids	20
1.4.1 Liquid/vapour interface – Aprotic ionic liquids	21
1.4.2 Liquid/vapour interface – Protic ionic liquids	22
1.4.3 Influence of water on IL structure	23
1.5 Thesis outline	24
1.6 References	26
Chapter 2: Experimental	37
2.1 Neutral impact collision ion scattering spectroscopy	37

2.1.1	Background	37
2.1.2	NICISS theory	39
2.1.3	Experimental setup	46
2.1.4	Targets	48
2.2	Electron spectroscopy methods	55
2.2.1	X-ray photoelectron spectroscopy	55
2.2.2	Ultra-violet photoelectron spectroscopy	56
2.2.3	Meta-stable induced electron spectroscopy	56
2.2.4	Experimental setup	57
2.3	Thin film pressure balance	59
2.3.1	TFPB theory	59
2.3.2	Experimental setup	60
2.4	Surface tension	62
2.4.1	Theory	62
2.4.2	Experimental setup	62
2.5	Molecular orbital calculations	63
2.5.1	Calculations	63
2.6	Sample preparation	64
2.6.1	Materials	64
2.6.2	Foam film holders	65
2.7	References	67
Chapter 3: Effect of the aliphatic chain length on electrical double layer formation at the IL/vacuum interface		71
3.1	Introduction	71
3.2	Results and Discussion	73
3.2.1	NICIS spectra	73
3.2.2	Deconvolution	76
3.2.3	Surface charge and electrical double layer	78
3.3	Conclusions	82
3.4	References	84
Chapter 4: Effect of water on the charge distribution at the surface of [C₆mim][Cl]		89
4.1	Introduction	89
4.2	Experimental	91
4.2.1	Materials	91
4.2.2	Experimental setup	92

4.3	Results and discussion	93
4.3.1	NICIS Spectra	93
4.3.2	Deconvolution	96
4.3.3	Effect of water	98
4.4	Conclusion	100
4.5	References	101
Chapter 5: Comparing the charge distribution along the surface normal in the [C₆mim]⁺ ionic liquid with different anions		105
5.1	Introduction	105
5.2	Results and discussion	106
5.2.1	NICIS Spectra	106
5.2.2	Comparing ion depth profiles	109
5.3	Conclusion	111
5.4	References	112
Chapter 6: Composition of the Outermost Layer and Concentration Depth Profiles of Ammonium Nitrate Ionic Liquid Surfaces		115
6.1	Introduction	115
6.2	Experimental	117
6.3	Results and Discussion	118
6.3.1	Outermost surface layer composition	118
6.3.2	Concentration depth profiles	123
6.3.3	Surface structure of the ILs	126
6.4	Conclusions	127
6.5	References	128
Chapter 7: Deconvolution of NICISS profiles involving elements of similar masses		131
7.1	Introduction	131
7.2	Experimental	132
7.3	Results and Discussion	133
7.3.1	NICISS profiles	133
7.3.2	Deconvolution	134
7.4	Conclusions	137
7.5	References	138
Chapter 8: Change of Surface Structure upon Foam Film Formation		141
8.1	Introduction	141
8.2	Experimental	143

8.3	Results and Discussion	143
8.4	Conclusions	148
8.5	References	149
Chapter 9: Effect of sodium halides on the surface structure of foam films stabilized by a non-ionic surfactant		151
9.1	Introduction	151
9.2	Experimental	153
9.2.1	Surface tension	153
9.3	Results and Discussion	154
9.3.1	Effect of salt on surfactant adsorption	154
9.3.2	Changes of the surface upon foam film formation	156
9.3.3	Preferential adsorption of ions at the foam film surface	157
9.3.4	Influence of salt on the thickness of foam films	160
9.4	Conclusions	162
9.5	References	164
Chapter 10: Conclusions		167

Abstract

In this work liquid systems containing ionic species are investigated in order to further understand the forces that govern the surface structure of liquids. The distribution of ions along the surface normal, or charge distribution, is especially important in foam films (such as soap bubbles) where the electrostatic forces generated from the separation of charges at the liquid/air interfaces play a pivotal role in stopping the film from collapsing.

Many powerful techniques for investigating surfaces require the samples to be measured under ultra-high vacuum. The volatile nature of liquids makes their use in these instruments difficult, especially so in the case of foam films which are already in a fragile, metastable state. Specialised equipment and experimental techniques are developed for the investigation of foam films under vacuum. A glass film holder is used to generate and hold the film. This film holder is held inside an enclosed cell designed to minimise the evaporation of solvent from the film and aid film stability. Variations to the setup are designed and tested which allow for greater stability of the foam film, along with the means to measure the films under altering conditions.

Foam films of a cationic surfactant, hexadecyltrimethylphosphonium bromide, were investigated. A range of measurements were performed that demonstrated the thinning, and consequential surface rearrangement, of the foam film over time. These results also indicated a decrease in the surface potential upon foam film formation, partially owing to the reorientation of surfactant molecules at the surface.

Foam films containing a non-ionic surfactant, dodecyldimethyl phosphine oxide, were also investigated using the above technique. These films were studied with no added electrolyte as well as added salts, where the anion was varied. Comparing the concentration depth profiles of the foam films to the corresponding bulk liquid surfaces for the various systems studied allowed for the determination as to how the liquid surface changes upon foam film formation. It was found that the addition of salt increased the surfactant adsorption at the surface of both the foam film and bulk liquid. Additionally, it was seen that while iodide was detected as a surface excess at the bulk liquid, chloride was not. Both are detected as a surface excess at the foam film surface.

Surfaces of ionic liquids were also investigated, as they represent a unique situation of a liquid being comprised totally of charged species. Thus, the charge distribution is not mediated by an additional species, as is the case with aqueous solutions. The effect of small amounts of water as a surface impurity in [C₆mim][Cl] was investigated. Increasing the water content lead to an increase in the amount of anion adsorbed at the surface, indicating how forces other than the electrostatic interaction between ions governs surface structure. It was seen that for both protic and aprotic ionic liquids that the cation aliphatic chain length had a significant influence on the surface structure. Increasing the chain length caused increased adsorption of the cation, with subsequent cation reorientation at the surface.

Declaration

I certify that this thesis does not incorporate without acknowledgement any material previously submitted for a degree or diploma in any university; and that to the best of my knowledge and belief it does not contain any material previously published or written by another person except where due reference is made in the text.

Christiaan Ridings

Acknowledgements

This thesis, and the entire journey of my PhD, would not have been possible without many different people.

Firstly, I would like to deeply thank my supervisor, Gunther Andersson. Having worked in his group for the last 5 and a half years, I have become enormously grateful for the opportunity to learn from such a dedicated professional, and work alongside a truly good person. Gunther has always provided me with advice, encouragement, and enthusiasm which gave me faith in my abilities that I might not otherwise have had. His ability to be so professional and so personable at the same time is outstanding.

I would like to thank the awesome people around Flinders University who have made this time both informative and enjoyable. My research group in particular has been a highlight: Anirudh Sharma, Natalya Schmerl, Alex Sibley, Ben Chambers, Herri Trilaksana, and Rantej Kler, along with others who have drifted through over the years. Other academics around the university, Prof. Joe Shapter, Prof. Jamie Quinton, Prof. David Lewis, Dr. Chris Gibson, have been a great source of advice over the years, even with matters not related to this project. I would like to specifically thank Assoc. Prof. Martin Johnston as his knowledge of organic chemistry and all things related has been a huge help to me. Thanks also to the other PhD students who have made this time what it is: Daniel Gruszecki, Daniel Mangos, Daniel Tune, Sam Ogden. I would like to specifically thank my office mate, Ashley Slattery. Working in different groups on completely different projects has given me a wider outlook on science, and it has been great to chat about all things over the years.

The Technical Services Unit at the university have been invaluable throughout my project. They have provided countless hours of assistance for maintenance as well as unit design and construction for the various little projects and ideas I've had over the years. Thanks to Bill Drury, Chris Price, Andrew Dunn, and Mark Ellis. In particular thanks to Wayne Peacock and Bob Northeast who I ended up bugging for help the most, but have also been great to chat to over the last few years.

I have been privileged to work with many great scientists over the last few years, and would like to thank those who have had significant impact on this project. Thanks to Prof. Cosima Stubenrauch, and Dr. Enda Carey, who facilitated my stay in Stuttgart and were able to provide me with great training and discussions during this time. I would like to thank Prof. Greg Warr for his fantastic assistance with synthesising and understanding protic ionic liquids, Dr. Ekaterina Pas for many fruitful discussions concerning molecular orbital calculations, and Dr. Vera Lockett for her assistance and ideas with the studies of aprotic ionic liquids.

I especially acknowledge those outside of the academic sphere who have helped me along the way. Thanks to all my great mates who have helped me to relax, unwind, and given me energy to keep going. Thanks to the Haig family in particular for basically having to put up with me like the rest of my family. To my amazing family, Dad, Mum, Khali, Shanna, Ollie, and Darryl, thanks for putting up with my frustrations at home and providing me with so much love and support along the way. Finally, I owe my deepest gratitude to Melanie. Your constant happiness, enthusiasm, and love have not only helped me through this time but made me want to keep improving in every way.

List of publications

Peer-reviewed journals

- [1] Ridings, C. & Andersson, G. Determining concentration depth profiles of thin foam films with neutral impact collision ion scattering spectroscopy. *Review of Scientific Instruments* **81**, 113907-113915 (2010).
- [2] Ridings, C., Lockett, V. & Andersson, G. Effect of the aliphatic chain length on electrical double layer formation at the liquid/vacuum interface in the [C_nmim][BF₄] ionic liquid series. *Physical Chemistry Chemical Physics* **13**, 17177-17184 (2011).
- [3] Ridings, C., Lockett, V. & Andersson, G. Significant changes of the charge distribution at the surface of an ionic liquid due to the presence of small amounts of water. *Physical Chemistry Chemical Physics* **13**, 21301-21307 (2011).
- [4] Wakeham, D., Niga, P., Ridings, C., Andersson, G., Nelson, A., Warr, G., Baldelli, S., Rutland, M., Atkin, R. Surface structure of a "non-amphiphilic" protic ionic liquid. *Physical Chemistry Chemical Physics* **14**, 5106-5114 (2012).
- [5] Ridings, C., Lockett, V. & Andersson, G. Comparing the charge distribution along the surface normal in the [C₆mim]⁺ ionic liquid with different anions. *Colloids and Surfaces A: Physicochemical and Engineering Aspects* **413**, 149-153 (2012).
- [6] Ridings, C., Warr, G. G. & Andersson, G. G. Composition of the outermost layer and concentration depth profiles of ammonium nitrate ionic liquid surfaces. *Physical Chemistry Chemical Physics* **14**, 16088-16095 (2012).
- [7] Andersson, G. & Ridings, C. Ion Scattering Studies of Molecular Structure at Liquid Surfaces with Applications in Industrial and Biological Systems. *Chemical Reviews* **114**, 8361-8387 (2014).
- [8] Ridings, C. & Andersson, G. G. Deconvolution of NICISS profiles involving elements of similar masses. *Nuclear Instruments and Methods in Physics Research Section B: Beam Interactions with Materials and Atoms* **340**, 63-66 (2014).

[9] Ridings, C., Stubenrauch, C. & Andersson, G. Effect of Sodium Halides on the Surface Structure of Foam Films Stabilized by a Nonionic Surfactant. *The Journal of Physical Chemistry C* **119**, 441-448 (2014).

[10] Ridings, C. & Andersson, G. Change of Surface Structure upon Foam Film Formation. *ChemPhysChem* **Accepted for publication** (2014).

DOI: 10.1002/cphc.201402821R1

Book chapters

Ridings, C. & Andersson, G. in *Innovations in Nanomaterials*, **Under review**, (Nova Science Publishers, Inc., 2014).

List of figures

- Figure 1-1.** Schematic illustration of the Gibbs dividing plane as adapted from Adamson.²⁰ The dividing plane is chosen such that Γ_{solvent} is equal to zero. For the solute (blue), the area to the right of the plane minus the area to the left gives a positive area, indicating a surface excess of solute..... 5
- Figure 1-2.** A picture of a typical liquid foam (left) along with a schematic illustration of an individual foam film (right). 13
- Figure 1-3.** *Left:* an illustration of a CBF (top) and NBF (bottom). *Right:* Schematic representation of a disjoining pressure curve, highlighting the contribution of different forces and the regions of CBF and NBF formation. 16
- Figure 2-1.** Schematic of the elastic scattering process. 40
- Figure 2-2.** Data evaluation of a NICIS TOF spectrum where the measured spectrum, hydrogen background, photon peak, and individual steps of the elements are shown.43
- Figure 2-3.** NICISS schematic (top down view)..... 46
- Figure 2-4.** Picture of the NICISS setup at Flinders University (taken circa January 2013). 46
- Figure 2-5.** NICISS sample targets (side view). (A) Solid sample holder consisting of an electrically isolated, rotating steel disc; (B) Gas phase target where a gas can be introduced into the chamber via a leak vale; and (C) Liquid sample target where the rotating steel disc is immersed into a reservoir containing the liquid. 48
- Figure 2-6.** Picture of a film holder used in the NICISS foam film experiments. ... 50
- Figure 2-7.** Schematic illustration of the latest foam film target (top). The film holder is connected to the reserve solution in the syringe by tubing. The cover attaches to the pressure cell and once the film holder is aligned, only the film over the aperture is seen through the front cover slit. Top down view of the foam film target (bottom) which displays the alignment with the ion beam..... 51
- Figure 2-8.** Normalized pressure through the aperture. Negative values of z indicate the inside of the pressure cell, i.e., towards the target. 52

Figure 2-10. Deexcitation mechanisms of a metastable atom via resonance ionisation (a ₁) followed by Auger neutralisation (a ₂) and via Auger deexcitation (b) on an insulator surface. Modified from Harada et al. ³³	57
Figure 2-11. Top-down schematic of the MIES rig at Flinders University. Some additional components that were not used in this thesis are not shown.....	58
Figure 2-12. Schematic illustration of the TFPB setup.....	60
Figure 3-1. NCISS TOF spectra of the ILs [C ₆ mim] [BF ₄], [C ₈ mim] [BF ₄], and [C ₁₀ mim] [BF ₄]. The spectra are offset for clarity. The vertical lines show the onsets for the elements in the TOF spectra, as indicated.....	74
Figure 3-2. Comparing the measured concentration depth profiles of: (a) carbon, (b) nitrogen, and (c) fluorine in the three ILs. Increasing depth values indicates the direction further towards the bulk, with zero being the outermost layer.	75
Figure 3-3. Measured, deconvoluted and fit to the measured concentration depth profiles of (a) nitrogen and (b) fluorine in the [C ₁₀ mim][BF ₄] IL. The data points shown in (a) are a sum of five measured data points.	76
Figure 3-4. Comparing the deconvoluted profiles of (a) nitrogen and (b) fluorine for all three ILs investigated.....	77
Figure 3-5. Comparing the deconvoluted anion (fluorine) and cation (nitrogen) concentration depth profiles and the space charge for (a) [C ₆ mim][BF ₄], (b) [C ₈ mim][BF ₄] and (c) [C ₁₀ mim][BF ₄].	79
Fig. 3-6. Schematic illustrating the surface orientation and distribution of the cation and anion in the three ILs as interpreted from the concentration depth profiles.	80
Figure 4-1. NCISS TOF spectra of [C ₆ mim][Cl] measured at the three different vacuum exposure times. The lines mark the TOF onset for the respective elements. The spectra are vertically offset for clarity.....	93
Figure 4-2. Concentration depth profiles as measured of (a) carbon, (b) nitrogen and (c) chloride at each of the three vacuum exposure times.	95
Figure 4-3. Measured, deconvoluted, fitted chloride concentration depth profiles and residua at (a) 1 hour and (b) 20 hours exposure to vacuum.....	96

Figure 4-4. Comparing the deconvoluted chloride concentration depth profiles at vacuum exposure times of 1 and 20 hours. The error bars are due to the uncertainty of the deconvolution procedure.....	97
Figure 5-1. NCISS TOF spectra of [C ₆ mim][Cl] and [C ₆ mim][BF ₄]. The spectra are vertically offset for clarity. [C ₆ mim][Cl] data as seen in Chapter 4 and [C ₆ mim][BF ₄] data as seen in Chapter 3.	107
Figure 5-2. Concentration depth profiles as measured of (a) carbon and (b) nitrogen for both of the ionic liquids studied, and (c) chloride for [C ₆ mim][Cl] and (d) fluorine for [C ₆ mim][BF ₄]. Concentrations have been normalised to the bulk values of concentration for each individual element. [C ₆ mim][Cl] data as seen in Chapter 4 and [C ₆ mim][BF ₄] data as seen in Chapter 3.	108
Figure 5-3. Deconvoluted concentration depth profiles of the anions in the two ionic liquids. Concentrations have been normalised to the bulk values of concentration for the individual elements (Cl and F). [C ₆ mim][Cl] data as seen in Chapter 4 and [C ₆ mim][BF ₄] data as seen in Chapter 3.....	110
Figure 6-1. Structure of the ions constituting the three ionic liquids, where grey is carbon, blue is nitrogen and red is oxygen.	118
Figure 6-2. MIE and UP spectra of the three ILs studied on binding energy scale along with MO eigenvalues. MOs were assigned to either the cation (+), anion (-) or undefined (+/-) with the aid of MO visualisation. Samples of MO images are provided for the different assignments.	119
Figure 6-3. MIE spectra of the three ILs along with the calculated MO eigenvalues and the Gaussian functions used to account for the MOs in the spectra.	120
Figure 6-4. Normalised elemental depth profiles of the three ILs investigated. The carbon profiles show a clear excess at the surface in EtAN that is not seen in EAN or PAN. Additionally, both nitrogen and oxygen are seen to be depleted at the surface of EtAN compared to EAN and PAN.....	123
Figure 6-5. Concentration depth profiles of the cationic ammonium, anion and cation alkyl chain in each of the three ILs investigated. The profiles indicate that while the surface of EAN is an homogenous distribution of the cation and anion, PAN shows an	

increased orientation of cation alkyl chains protruding from the surface, while EtAN shows a clear excess of the cation chain. 124

Figure 7-1. NICIS spectra on the TOF scale for the 4 solutions investigated. The onset for the step of each element is indicated by a vertical line. The spectra are vertically offset for clarity. 133

Figure 7-2. Concentration depth profile of phosphorus for the 4 systems investigated on the energy scale. The vertical dashed lines indicate the energy for zero depth of the respective element, with decreasing energy indicating increasing depth towards the bulk. The increased concentration of the 10 mM NaCl profile between the Cl and P onset compared to the other systems is a possible indication of the detection of Cl. 134

Figure 7-3. Deconvoluted P/Cl profile of the 0.1 mmol/kg NaCl solution with both the energy scale and the depth scale for P indicated. A deconvoluted profile is determined using a genetic algorithm, and then convoluted to produce the fit to the measured profile. The standard deviation of all data sets to the final averaged profile (deconvoluted) gives the error bars for the deconvolution. 135

Figure 7-4. Deconvoluted profiles of the four systems studied. The energy corresponding to zero depth for Cl is 1759 eV, as indicated by the dashed line. The profiles at lower energies correspond to P. The depth scale from 0 to 10 Å is given for both P and Cl as indicated by the horizontal bars. 136

Figure 8-1. NICISS time-of-flight spectrum of the glycerol / C16TPB system from the liquid surface and foam film surface. The vertical lines indicate the onset of the step for the respective element, while the spectra have been vertically offset for clarity.... 143

Figure 8-2. Concentration depth profiles of carbon and oxygen from the foam film. Subtracting the profile of oxygen from that of carbon leaves only the carbon due to the surfactant. 145

Figure 8-3. Concentration depth profiles of the anion, cation and surfactant alkyl chain of the C16TPB in glycerol for the surface of the bulk solution (left panel) and the foam film (right panel). 146

Figure 8-4. Comparing the concentration depth profiles between the ‘bulk’ and film surface for the surfactant ‘alkyl’ (top), phosphorus headgroup (middle), and bromide anion (bottom). 147

Figure 8-5. Deconvoluted profiles for P at the bulk liquid and foam film surface (left) and Br at the bulk liquid and foam film surface (right). The Br profiles have been adjusted by a factor such that charge neutrality is observed between the cation and anion.	148
Figure 9-1. Surface tension as a function of concentration for the glycerol / C ₁₂ DMPO system.	153
Figure 9-2. NICISS spectra of glycerol / C ₁₂ DMPO / 7.90 mM NaI for both the foam film and bulk liquid surface. Spectra are shown on the time of flight scale, and are vertically offset for clarity. The onsets for the steps of each element are indicated by the dashed lines.....	154
Figure 9-3. Concentration depth profiles of phosphorus at the glycerol / C ₁₂ DMPO bulk liquid surface with no added salt, added NaCl, and added NaI. Both salt concentrations are 7.90 mM.....	155
Figure 9-4. Concentration depth profiles of phosphorus as measured. Comparison of the P profiles of glycerol / C ₁₂ DMPO / NaI films with NaI concentrations as indicated (left), and of glycerol / C ₁₂ DMPO / 7.90 mM salt films with the salt as indicated (right).....	156
Figure 9-5. Comparison of the alkyl chain profile and P profile at the surface of the bulk liquid (left) and foam film (right) in the glycerol / C ₁₂ DMPO system. The shift of P away from the surface in the film compared to the bulk indicates a change in orientation of the surfactant in the foam film.....	157
Figure 9-6. NICISS spectra of pure glycerol, glycerol / NaI, and glycerol / C ₁₂ DMPO / NaI with both NaI concentrations at 7.90 mM. Spectra are shown on the time of flight scale, and are vertically offset for clarity.....	157
Figure 9-7. Comparison of the concentration depth profiles of iodide for the system glycerol / C ₁₂ DMPO / 7.90 mM NaI at the surface of the bulk liquid and the surface of the foam film (left). Concentration depth profiles of iodide at the foam film surface for three different NaI concentrations (right).	158
Figure 9-8. Concentration depth profile of P for the glycerol / C ₁₂ DMPO system at the bulk liquid surface (left) and foam film surface (right). Due to their similar masses, the signals for Cl ⁻ and P are hardly distinguishable (see text for further details). Cl ⁻ should appear at a slight negative depth on the P depth scale, which is seen in the foam film as the	

increased concentration at negative depths in the 7.90 mM system. This presence of Cl^- is not detected at the bulk liquid surface. 159

Figure 9-9. Deconvoluting the P/Cl^- profiles allows for the separation of the profiles of the two elements. This result shows that Cl^- is present as a detectable surface excess in the foam films. 160

Figure 9-10. Disjoining pressure curves for the water / C_{12}DMPO system with no salt, 0.1 mM NaI , and 0.1 mM NaF . DLVO fits to the data are shown as dotted lines, with the resulting surface charge given in the legend. 161

List of tables

Table 2-1. Different methods of ion scattering spectroscopy, which utilise differences in probing techniques and what they detect to gain different information about surfaces.	38
Table 2-2. Equivalent liquid layer thicknesses for two solvents given a path length of 10mm and temperature of 293K. P_{vap} is the vapour pressure and ρ_{liquid} is the liquid density. ²⁵	53
Table 3-1. Depth of maximum concentration for fluorine (F, anion) and nitrogen (N, cation). The error for each position falls within the given range but is the same for both elements in all ILs measured. Additionally, the depth of maximum concentration for nitrogen in [C ₆ mim][BF ₄] was determined as -1 Å in the deconvoluted profile. However as this has no physical meaning, the value is set to 0 Å (outermost layer). This change is less than the error in determining the zero mark.	78
Table 4-1. Water content as obtained from KF titration at different exposure times to vacuum.....	92
Table 6-1. Surface composition ratios, I_{norm} , derived from MIES and UPS, together with spectral data used in the determination.....	122

Abbreviations

Abbreviations

AIL	Aprotic ionic liquid
CBF	Common black film
cmc	Critical micelle concentration
DLVO (theory)	Derjaguin Landau Verwey Overbeek (theory)
DRS	Direct recoil spectroscopy
EDL	Electrical double layer
FPDT	Foam pressure drop technique
FWHM	Full-width half-maximum
HOMO	Highest occupied molecular orbital
IL	Ionic liquid
IMFP	Inelastic mean free path
ISS	Ion scattering spectroscopy
LEIS	Low energy ion scattering
MD	Molecular dynamics
MIES	Metastable induced electron spectroscopy
MO	Molecular orbital
NBF	Newton black film
NICISS	Neutral impact collision ion scattering spectroscopy
NLO	Non-linear optical
NMR (spectroscopy)	Nuclear magnetic resonance (spectroscopy)
NR	Neutron reflectivity
PIL	Protic ionic liquid
QMS	Quadrupole mass spectrometer
RBS	Rutherford backscattering spectroscopy

RTIL	Room temperature ionic liquid
SFA	Surface force apparatus
SFG	Sum frequency generation vibrational spectroscopy
TFPB	Thin film pressure balance
TOF	Time of flight
UHV	Ultra high vacuum
UPS	Ultraviolet photoelectron spectroscopy
VSFS	Vibrational sum frequency spectroscopy
XPS	X-ray photoelectron spectroscopy
XR	X-ray reflectivity

Frequently discussed chemical abbreviations

C _n TAB	(alkyl)trimethylammonium bromide
C _n TPB	(alkyl)trimethylphosphonium bromide
C ₁₂ DMPO	(alkyl)dimethylphosphine oxide
[C _n mim] ⁺	1-(alkyl)-3-methylimidazolium ⁺
[BF ₄] ⁻	tetrafluoroborate ⁻
POPC	1-palmitoyl-2-oleoylphosphatidylcholine
EAN	ethylammonium nitrate
PAN	propylammonium nitrate
EtAN	ethanolammonium nitrate

Contextual Statement

This thesis presents the investigations into the surface structure of liquids containing ionic species as performed as part of the author's PhD project. It also contains some grounding work from the author's preceding Honours project that directly flows onto the PhD project, which justifies its inclusion.

The Introduction chapter contains a literature review of the current field directly concerning the project, while the Experimental chapter contains the experimental details of the project, along with a discussion of the experimental methods used as part of the project. Given that such a large portion of the project was involving the NICISS technique, a particularly in-depth discussion and review of the method is given in that chapter.

The results chapters 3 – 7 are reformatted versions of the published peer-reviewed papers of the same title, while chapters 8 and 9 are reformatted versions of papers either under review or sent to journals for review.

The author of this thesis was the primary author of all papers used as results chapters. All experimental work was completed by the author. Exceptions involve: Dr. V. Lockett who carried out the Karl Fisher titration to determine the water content in the aprotic ILs; and Dr. E. Carey who performed TFPB measurements (in addition to those completed by the author) in order to test data reproducibility. The author also completed all data evaluation, but acknowledges the input of the respective co-authors in the final interpretation of results.

